JCTC Journal of Chemical Theory and Computation

Article

pubs.acs.org/JCTC

Extension of the Universal Force Field to Metal–Organic Frameworks

Matthew A. Addicoat,† Nina Vankova,† Ismot Farjana Akter, and Thomas Heine*

School of Engineering and Science, Jacobs University Bremen Campus Ring 1, 28759 Bremen, Germany

Supporting Information

ABSTRACT: The Universal Force Field (UFF) (Rappé et al., *J. Am. Chem. Soc.* **1992**) provides a general approach to molecular mechanics for molecules and materials composed of elements throughout the periodic table. Though the method is tunable by the specification of bond orders and the introduction of effective charges, the presently available list of atom types is insufficient to treat various systems containing transition metals, including metal–organic frameworks (MOFs). As MOFs are composite materials built of a combination of individually stable building blocks, a plethora of MOF structures are possible, and the prediction of their structure with a low-cost method is important. We have extended the UFF parameter set to include transition metal elements Zn, Cu, Ni, Co, Fe, Mn, Cr, V, Ti, Sc, and Al, as they occur in MOFs, and have proposed additional O parameters that provide reliable structures of the metal oxide clusters of the connectors. We have benchmarked the performance of the MOF extension to UFF (UFF4MOF) with respect to experimentally available data and to DFT calculations. The parameters are available in various well-spread programs, including GULP, deMonNano, and ADF, and all information is provided to include them in other molecular mechanics codes.

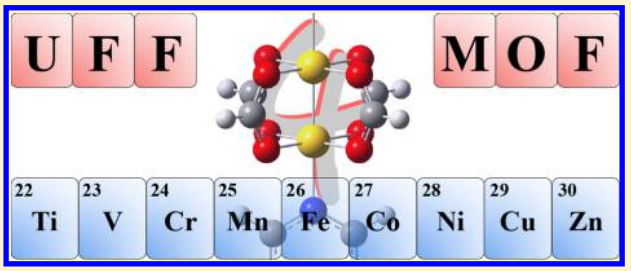

1. INTRODUCTION

The past decade has seen an enormous success in synthesis and characterization of crystalline framework materials, where building blocks are stitched together by strong coordinative or covalent bonds. Most notable are metal–organic frameworks (MOFs) in which typically polyatomic inorganic metal-containing clusters (connectors) are linked by organic molecular bridges (linkers).[1] Over a decade ago, Yaghi et al.[2] introduced the concept of reticular chemistry, where MOFs could be designed and synthesized in a rational way from different combinations of molecular building blocks. The combination of the metal ions or metal-oxide clusters and the organic linkers in MOFs provides endless possibilities to create materials with various topologies, structures, and elemental compositions, and hence with different mechanical and electronic properties and applications.

MOFs have rapidly become a prominent and burgeoning area of research due to the fact that these highly porous and highly ordered materials can be used for applications as wide-ranging as gas storage, liquid-phase sorption and separation,[3] catalysis,[3d−f,4] magnetism,[3e,5] sensing,[6] thin films,[7] proton conduction,[8] drug delivery,[9] and many more. Besides the many experimental syntheses and applications, most of which include computational analysis, many hypothetical structures have also been reported.[10] An increasing focus in computational MOF research is the targeted pre-synthesis design of frameworks with specific given properties. Such computational design involves the screening of the many millions of possible MOFs in order to search for the most suitable ones, and ideally results in the rational suggestion of only a handful of likely candidates for attempted synthesis.

As the building blocks of MOFs typically comprise 10–30 atoms, unit cells quickly get very large, containing hundreds or even thousands of atoms. Such large unit cell sizes limit the computational methods that can be used to investigate these materials. Even parametrized *ab initio* methods such as Density Functional based Tight Binding (DFTB)[11] may take hours to compute a single structure, limiting their usefulness in screening large numbers of structures. In this case, one therefore resorts to force field (FF) methods.

Unfortunately, many of the popular force fields such as MM2,[12] MM3,[13] AMBER,[14] and CHARMM[15] are limited to particular combinations of atoms or strongly fit for particular types of structures (e.g., proteins,[14] zeolites,[16] liquid mixtures[17]). It is subsequently difficult to apply these force fields to other molecular systems.

Of relevance to the description of MOFs *via* molecular mechanics approaches are the force fields parametrized for metalloporphyrines, in which a transition-metal ion is coordinated to heterocyclic organic ligands. For example, MM2(87) FF parameters have been developed for iron porphyrins with Fe^{II} or Fe^{III} in various spin states and coordination,[18] and later on, for Co^{III} corrinoids.[19] It has been found that a unique set of parameters is insufficient to describe the different forms of iron in the considered porphyrins and that each type of Fe ion requires its own set of parameters.[18] The CHARMM and AMBER FFs have been extended to describe the partial charges and geometries of heme in both redox states.[20] A third example is the FF of Spiro

Received: October 31, 2013
Published: January 20, 2014

and co-workers,[21] which has been developed to reproduce vibrational features (frequencies and isotope shifts) of Ni^{II} porphyrin derivatives (NiP, NiTPP, and NiOP).

Several researchers have begun to parametrize force fields for MOFs: first principles derived force fields have been developed for predicting the structure of MOF-5,[22] the Cu-paddlewheel based MOFs[23] and MIL-53(Al),[24] as well as for describing diffusion of guest molecules[22a,25] and gas sorption properties of MOFs.[26] While these force fields yield highly accurate structures, and even properties such as vibrational frequencies, thermal expansion behavior and self-diffusion coefficients, they suffer from a lack of transferability. Recent work toward more transferable parameters includes a first-principles derived force field, MOF-FF, which has been parametrized for several MOF-families including IRMOFs, UiO, as well as Cu- and Zn- based paddlewheel frameworks (with and without pillar ligands).[27] Another approach is to accept the nontransferability of parameters but automate their generation.[28]

At the other end of the specificity/applicability spectrum are approaches such as the Universal Force Field (UFF)[29] that promise essentially complete coverage of the periodic table. Such a universal approach suffers the disadvantage of only providing moderate accuracy for any given system but possesses the corresponding advantage that it may be applied broadly.

UFF as defined by Rappé,[29] with recently revised parameters for intermolecular interactions,[30] includes both connectivity-based (valence) and nonbonded parameters: Connectivity-based parameters are the coordination number, the effective charge, effective covalent radius, and bond angle. The bond length between any two atoms i and j, r_{ij}, is corrected by a factor (eq 2 in ref 29) that includes the contribution of a user-supplied bond-order (i.e., double, triple, resonant...). Non-bonded parameters include the Lennard-Jones potential parameters and a scaling parameter ζ that allows fine-tuning the shape of the potential. For most elements, a value of $\zeta = 12$ is chosen, coinciding with the Lennard-Jones potential.

In the over 20 years since its introduction, UFF has been applied to systems ranging from main group compounds,[31] organic molecules,[32] metal complexes[33] and even MOFs.[34] However, the existing parameters generally fail to reproduce the unique coordination environments typical of the metal-containing secondary building units (SBUs) of MOFs.

In this paper, we present a set of tuned parameters designed to extend UFF for the calculation of framework materials. These additional 18 atom types can be easily incorporated in any software that includes an UFF module. We call this extension of UFF atom types that are optimized for MOFs "UFF4MOF". The additional UFF4MOF atom types are distinct from and complementary to the atom type table provided initially by Rappé et al.[29] Note that our UFF4MOF parameter extension is designed to permit calculation of structures that are not possible employing only the standard UFF parameters. In this work, we fit and test the UFF4MOF parameters. The original force field definition and parameters remain unchanged, and the UFF4MOF parameters complement, but never replace, the parameters of Rappé et al. Therefore, we will use the term "UFF" in the remainder of this work, as shorthand for a "UFF calculation with the standard UFF and additional UFF4MOF parameters".

Besides introducing new atom types, we further recommend bond orders, which describe well the molecular geometry of individual SBUs that are typical of MOFs. Next, we validate the ability of the extended UFF4MOF parameters to reproduce structures and topologies of prototypical framework materials by comparing the predicted lattice parameters to available experimental data for representatives of several MOF families, including IRMOFs,[35] MOF-177,[36] MIL-53,[37] HKUST-1,[38] DMOF-1,[39] MFU-4, and MFU-4*l*,[40] as well as MOF-235[41] and $Ni_2(bdc)_2(dabco)$.[38c]

2. COMPUTATIONAL METHOD

The UFF calculations were carried out using deMonNano[42] and GULP.[43] Preliminary tests (see Supporting Information) showed that the geometries of the organic linkers are well described using standard UFF parameters and typical (i.e., single, double, triple, resonant) bond orders in accord with "chemical intuition", and therefore, we focus solely on the metal-containing SBUs.

A training set of SBUs, representative of the connectors commonly employed in MOFs, was compiled. This set includes $Zn_4O(CO_2)_6$ (SBU of IRMOFs, MOF-177, and others), oxo-centered trimers (SBU of MIL-100, MIL-101, MOF-235), the MIL-53-type SBU, paddlewheels (SBU of HKUST-1, DMOF-1, SURMOFs) and Kuratowski-type SBU (as in MFU-4 and MFU-4*l*). All SBUs were calculated as isolated gas-phase molecules and saturated, where necessary, with hydrogen atoms.

Following the general UFF convention that nonbonded parameters and effective charge are identical for each atom type, we employ these parameters directly from the standard UFF[29] and only the coordination number, covalent radius, and angle need to be determined. In practice, the coordination number and bond angle are readily determined by observation and therefore only the covalent radius requires determination. For each combination of metal and SBU geometry in the training set, the covalent radius of the metal was scanned in 0.02 Å increments from 0.9 to 1.7 Å and the geometry of the SBU was optimized using the normal, nonperiodic optimizer, with default cutoffs on energy and gradients. Geometric parameters were extracted from the optimized geometries and the covalent radius was chosen to minimize the residual error between the UFF and reference geometries. In order to accurately reflect SBU geometries, two new oxygen types are introduced as "hybrids" of existing oxygen types, no further refinement of the oxygen covalent radius was attempted in these cases. The new atom types are labeled following the five-character mnemonic label convention of UFF.

For inorganic connectors of the type $Zn_4O(CO_2)_6$, oxo-centered trimers, MIL-53, and MFU-4, we considered high quality experimental structures as reference geometries. In the case of paddlewheel SBUs (PWs), density-functional theory (DFT) was used to provide reference structures for the parameter optimization due to the lack of suitable and consistent experimental references for the whole series of divalent metal ions considered. The DFT calculations were carried out in ADF2012,[44] employing the Becke88-Perdew86 gradient-corrected density functional (BP86)[45] with Slater-type basis sets of triple-ζ plus polarization (TZP)[46] quality and the small core approximation. Scalar relativistic corrections were taken into account within the ZORA formalism.[47] Unless the spin state is specifically indicated, we use closed shell calculations.

Table 1. List of the New Force Field Parameters (UFF4MOF) Introduced to UFF

	valence[b]			nonbonded[c]			
new atom types[a]	bond r_i (Å)	angle θ_0 (deg)	coordination number	distance x_i (Å)	energy D_i kcal/mol	scale ζ	effective charge Z_i*
O_3_f	0.634	109.47	4	3.5	0.06	14.085	2.3
O_2_z	0.528	120.0	3	3.5	0.06	14.085	2.3
Al6+3	1.22	90.0	6	4.499	0.505	11.278	1.792
Sc6+3	1.44	90.0	6	3.295	0.019	12.0	2.595
Ti4+2	1.38	90.0	4	3.175	0.017	12.0	2.659
V_4+2	1.18	90.0	4	3.144	0.016	12.0	2.679
V_6+3	1.30	90.0	6	3.144	0.016	12.0	2.679
Cr4+2	1.10	90.0	4	3.023	0.015	12.0	2.463
Cr6f3	1.28	90.0	6	3.023	0.015	12.0	2.463
Mn6+3	1.34	90.0	6	2.961	0.013	12.0	2.43
Mn4+2	1.26	90.0	4	2.961	0.013	12.0	2.43
Fe6+3	1.32	90.0	6	2.912	0.013	12.0	2.43
Fe4+2	1.10	90.0	4	2.912	0.013	12.0	2.43
Co3+2	1.24	109.47	4	2.872	0.014	12.0	1.308
Co4+2	1.16	90.0	4	2.872	0.014	12.0	1.308
Cu4+2	1.28	90.0	4	3.495	0.005	12.0	2.43
Zn4+2	1.34	90.0	4	2.763	0.124	12.0	1.308
Zn3f2	1.24	109.47	4	2.763	0.124	12.0	1.308

[a]Notation of the new atom types. [b]Valence parameters: bond (covalent) radius, bond angle, and coordination number as determined in this work. [c]Nonbonded UFF parameters taken from ref 29. The table is given in the same format as the UFF parameters of Rappé's original work.[29]

3. RESULTS AND DISCUSSION

A summary of the new UFF4MOF atom types introduced in UFF is shown in Table 1.

3.1. $Zn_4O(CO_2)_6$ SBU. The $Zn_4O(CO_2)_6$ octahedron is undoubtedly one of the most widely used and studied SBUs in MOF chemistry, largely due to the extensive series of isoreticular MOFs (IRMOFs) of Yaghi and co-workers.[35] The crystallographically determined structure of this cluster comprises four tetrahedral zinc ions coordinated to six carboxylate groups and linked by a central tetrahedral oxygen atom, O_{cent} (Figure 1).

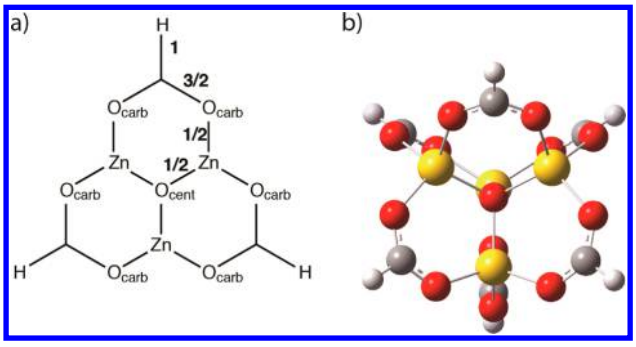

Figure 1. (a) Single-face schematic view of the $Zn_4O(CO_2H)_6$ model cluster with bond orders used in the UFF calculations. O_{cent} indicates central oxygen and O_{carb} indicates carboxylic oxygens. (b) Ball-and-stick representation of the $Zn_4O(CO_2H)_6$ structure as predicted by UFF with parameter extension for MOFs. H atoms added for saturation. Color legend: Zn yellow, O red, C gray, and H white. For the choice of UFF atom types, see Table 2.

To calculate the structure of this SBU, we introduced two new atom types, namely Zn3f2 for describing the tetrahedrally coordinated Zn^{II} ions and O_3_f suited for the central tetrahedral oxygen. In both notations "f" stands for atoms in framework materials. The new atom type Zn3f2 differs from the UFF standard Zn3+2 solely in the value of the bond radius, which is 0.05 Å larger for the new atom type. However, this small change leads to significantly improved geometry of the $Zn_4O(CO_2)_6$ SBU (see below). The O_3_f atom type has the same covalent radius as the UFF-defined O_2 (r_i = 0.634 Å) but differs from O_2 in bond angle (θ_0 = 109.47°) and coordination number (4); see Table 1. For the remaining atoms, we adopted standard UFF parameters (O_2 for carboxylic oxygen O_{carb}, C_R for carbon and H_ for hydrogen[29]). To reflect the bonding situation, we employed bond orders of 3/2 for all C−O_{carb}, 1/2 for all Zn−O_{carb} and Zn−O_{cent}, and 1 for all C−H distances (Figure 1a). The predicted structure of the $Zn_4O(CO_2)_6$ SBU saturated with H atoms is depicted in Figure 1b. The performance of the method is shown in Table 2, which compares the calculated and the experimental values of selected bond lengths and angles.

It is clear from Table 2 that the UFF calculated structure of $Zn_4O(CO_2H)_6$ agrees very well with the experimental benchmark. The Zn−Zn distances and the Zn−O_{cent} bonds are underestimated by only 0.5%, the Zn−O_{cent}−Zn valence angle agrees exactly with the experimental value, and the largest deviations, as obtained for the Zn−O_{carb} distances and the Zn−O_{carb}−C angles, are around 1−2%. Not surprisingly, the same error range is obtained when comparing the UFF to the DFT data.

The use of the standard Zn3+2 instead of the new Zn3f2 parameter results in larger underestimation of the Zn−Zn and Zn− O_{cent} distances by 4% and 5%, respectively.

The so-derived combination of atom types and bond orders was employed to calculate the structures of MOF-5 (IRMOF-1) and several other members of the IRMOF family, as well as of MOF-177 (see Section 3.6).

3.2. Trimeric Oxo-centered SBU. The trimeric oxo-centered assembly with the general formula $M_3O(CO_2)_6$ has been experimentally realized in molecular complexes and/or framework compounds, with M corresponding to Al, Sc, V, Cr, Mn, and Fe. The crystal structure of this cluster consists of three trivalent metal ions, M^{III}, connected via six carboxylate groups and a central oxygen atom, O_{cent}, with trigonal-planar

dx.doi.org/10.1021/ct400952t | J. Chem. Theory Comput. 2014, 10, 880−891

Table 2. UFF Derived Structural Characteristics (Bond Lengths and Angles), Experimental,[35a] and DFT Reference Data and Calculated Errors for the $Zn_4O(CO_2H)_6$ SBU[a]

selected structural characteristics	UFF	experiment[b]	DFT[c]	% error w.r.t. experiment[d]	% error w.r.t. DFT[e]
Zn−Zn [Å]	3.165	3.18	3.20	*−0.47*	*−0.94*
$Zn-O_{cent}$ [Å]	1.94	1.95	1.95	*−0.51*	*−0.51*
$Zn-O_{carb}$ [Å]	1.98	1.94	1.98	*2.06*	*0.00*
$Zn-O_{cent}-Zn$ [deg]	109.5	109.5	109.6	*0.0*	*−0.1*
$O_{cent}-Zn-O_{carb}$ [deg]	111.5	111.3	111.9	*0.2*	*−0.3*
$Zn-O_{carb}-C$ [deg]	132.6	131.0	128.4	*1.2*	*3.3*
$O_{carb}-Zn-O_{carb}$ [deg]	107.3	107.6	106.8	*−0.3*	*0.5*

[a]Force field parameters employed were Zn3f2 for Zn^{II}, O_3_f for O_{cent} (UFF4MOF atom types, see Table 1); O_2 for O_{carb}, C_R and H_ (UFF atom types[29]); bond orders as shown in Figure 1a. [b]Taken from ref 35a. [c]Taken from DFT optimized structures. [d]Calculated as $(X_{UFF} - X_{Experiment})/X_{Experiment} \times 100$. [e]Calculated as $(X_{UFF} - X_{DFT})/X_{DFT} \times 100$, where X_{UFF} denotes UFF-predicted, $X_{Experiment}$ denotes experimental and X_{DFT} denotes DFT-predicted values of respective bond lengths and angles.

configuration (see Figure 2). The octahedral coordination environment of each M^{III} site is completed by an axially

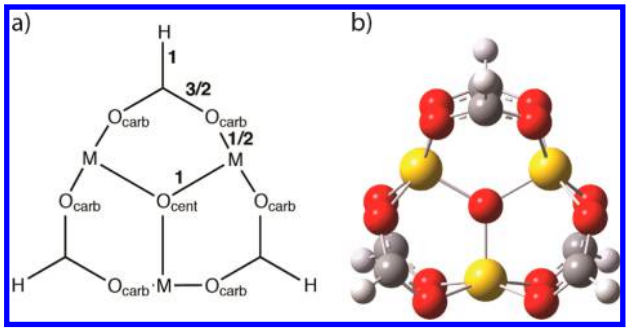

Figure 2. (a) Single-face schematic view of the $M_3O(CO_2H)_6$ model cluster with bond orders used in the UFF calculations. M indicates trivalent metal ions, O_{cent} is used for central oxygen, and O_{carb} for carboxylic oxygens. (b) Ball-and-stick representation of the $M_3O(CO_2H)_6$ SBU as predicted by UFF plus the UFF4MOF parameter extension. H atoms added for saturation. Color legend: trivalent metal ions M yellow, O red, C gray, and H white. UFF atom types are given in Table 3.

coordinated capping ligand, typically a solvent molecule. For the sake of simplicity, the capping ligands are not considered in our SBU model structures. The $M_3O(CO_2H)_6$ cluster has an overall charge of +1 that was neglected in the UFF calculations. We justify our neglect of charge in the UFF calculation of the isolated SBU by noting that (i) UFF charges are only defined for intermolecular interactions and interactions between third and higher neighbors and (ii) the same SBU appearing in different frameworks will have its formal charge compensated for to differing degrees by the framework ligands and coordinated solvent. In addition, within a periodic framework, the extended geometry of the framework maintains the local symmetry of the SBU, regardless of the location of the counterion. On the other hand, in a calculation of an isolated SBU, the inclusion of an explicit counterion will break the symmetry of the SBU. Considering the SBU as uncharged is therefore likely to result in the most broadly applicable parameters.

To describe the octahedrally coordinated M^{III} ions in the oxo-centered trimer, we introduced a set of new atom types, labeled M_6+3, for M = Al^{III}, Sc^{III}, V^{III}, Mn^{III}, and Fe^{III}. For Cr^{III}, we used a slightly different notation, Cr6f3, to distinguish the new parameter from the UFF-existing Cr6+3. The new atom type Cr6f3 differs from the UFF standard Cr6+3 solely in the value of the bond radius, which is 0.06 Å shorter for the new atom type. This small modification of the Cr atom type improves the UFF predicted results only slightly in the case of the oxo-centered Cr trimer but considerably in the case of the Cr-containing MIL53-type SBU (see Section 3.3). Each atom type from the M_6+3 series (Table 1) is characterized by the bond angle of 90°, coordination number of 6 and metal bond radius chosen with respect to a corresponding reference geometry. Additionally, for reflecting the trigonal-planar configuration of the central oxygen in $M_3O(CO_2H)_6$ that differs from the tetrahedral O_{cent} in the $Zn_4O(CO_2)_6$ SBU, we defined the O_2_z atom type with r_i = 0.528 Å, θ_0 = 120°, and coordination number of 3 (Table 1). In this respect, O_2_z represents a hybrid of the UFF-defined O_2 and O_3_z atom types (cf. Table 1 in ref 29). As in the case of the $Zn_4O(CO_2)_6$ octahedron, the existing UFF O_2, C_R and H_ atom types were found to perform reasonably well for the carboxylic oxygens (O_{carb}), carbons, and hydrogens in the oxo-centered trimer. The bonding situation was described using bond orders reflecting resonant $C-O_{carb}$ bonds, single $M-O_{cent}$ and C−H, and half $M-O_{carb}$ bonds (see Figure 2a). The UFF predicted structure of the $M_3O(CO_2H)_6$ SBU is shown in Figure 2b, and the calculated structural characteristics are presented in Table 3 along with the maximum percent errors with respect to the experimental reference data.

As can be readily seen in Table 3, the M−M and $M-O_{cent}$ distances are typically underestimated in the computed structure of $M_3O(CO_2H)_6$, and the largest errors are of about −4.5%, as obtained for Sc. The $M-O_{carb}$ bonds are, on the contrary, overestimated by the UFF calculations (except for $Al-O_{carb}$), with the maximum deviation of 3.6% found in the case of $V-O_{carb}$. The calculation of the Cr oxo-centered trimer employing the UFF Cr6+3 instead of the UFF4MOF Cr6f3 atom type results in larger overestimation of the $Cr-O_{carb}$ bond lengths (5.1% vs 2%). Importantly, UFF with our parameter extension is able to reproduce qualitatively the experimentally observed difference in the $M-O_{cent}$ and $M-O_{carb}$ bond lengths, the former being always shorter than the latter (Table 3). The agreement between predicted and experimental valence angles is excellent for all $\theta_0(M-O_{cent}-M)$ and reasonable for all other angles, with maximum errors of less than 5%.

The resulting atom types and bond orders were employed to simulate the structure of MOF-235 (see Section 3.6).

3.3. MIL-53 Type SBU. The MIL-53 class of materials developed by the Férey group[37a] have attracted intense research interest due to their breathing behavior and remarkable chemical robustness enabling a number of postsynthetic

Table 3. UFF Derived Structural Characteristics (Bond Lengths and Angles), Experimental Reference Data in Parentheses and Calculated Maximum Percent Errors for the Trimeric Oxo-centered SBU[a]

metal center	M−M [Å]	M−O_{cent} [Å]	M−O_{carb} [Å]	M−O_{cent}−M [deg]	O_{cent}−M−O_{carb} [deg]	M−O_{carb}−C [deg]	O_{carb}−M−O_{carb}(*trans*) [deg]
Al^{III}	3.16 (3.18)	1.82 (1.84)	1.89 (1.88−1.89)	120.1 (120.0)	95.6 (96.0)	134.2 (130.7−131.5)	169.1 (168.0)
Sc^{III}	3.34 (3.50)	1.93 (2.02)	2.14 (2.11)	120.0 (120.0)	95.3 (93.0)	133.8 (135.4)	169.6 (174.0)
V^{III}	3.21 (3.28)	1.85 (1.89)	2.03 (1.96)	120.0 (120.0)	96.2 (93.7)	133.0 (129.5)	167.9 (174.3)
Cr^{III}	3.20 (3.28)	1.85 (1.86)	2.01 (1.97)	120.0 (118.8)	96.1 (97.3)	133.3 (132.6)	168.1 (169.9)
Mn^{III}	3.26 (3.28)	1.88 (1.84−1.93)	2.06 (1.93−2.11)	120.0 (117.3−121.5)	95.7 (91.5−96.9)	133.6 (127.6−137.2)	168.9 (168.8−174.1)
Fe^{III}	3.27 (3.29)	1.89 (1.90)	2.07 (2.01)	120.1 (119.9/120.1)	95.6 (92.2−97.7)	133.6 (129.3−135.7)	168.9 (165.6−174.8)
max % error[b]	*−4.57*	*−4.46*	*3.57*	*1.0*	*2.7*	*2.7*	*−3.7*
for	Sc	Sc	V	Cr	V	V	V

[a]Force field parameters employed were M_6+3 for *M* = Al^{III}, Sc^{III}, V^{III}, Mn^{III} and Fe^{III}, Cr6f3 for Cr^{III}, O_2_z for O_{cent} (UFF4MOF atom types, see Table 1); O_2 for O_{carb}, C_R and H_ (UFF atom types[29]); bond orders as shown in Figure 2a. Experimental reference values taken from refs 48−53 for Al, Sc, V, Cr, Mn, and Fe, respectively. [b]The maximum % errors are derived after calculating all % errors for the $M_3O(CO_2H)_6$ series. The % errors are calculated as $(X_{UFF} - X_{Experiment})/X_{Experiment} \times 100$, where X_{UFF} denotes the UFF-predicted and $X_{Experiment}$ denotes the experimental values of respective bond lengths and angles.

modifications not applicable to other MOFs.[54] To treat the inorganic building block of MIL-53, we considered a finite cluster very similar to the model proposed by Vanduyfhuys and co-workers.[24] As shown in Figure 3, it represents a segment of a

Figure 3. (a) Single-face schematic view of the MIL-53 type model cluster with bond orders used in the UFF calculations. M indicates trivalent metal ions, O_{carb} is used for carboxylic oxygens and O_{hyd} for oxygens from the μ_2−OH bridges. (b) Ball-and-stick representation of the structure of the MIL-53 type SBU as predicted by UFF plus the UFF4MOF parameter extension. Color legend: trivalent metal ions M yellow, O red, C gray, and H white. UFF atom types are given in Table 4.

metal-oxide chain that consists of four corner-sharing MO_6 octahedra interconnected via μ_2−OH bridges and carboxylate groups of the 1,4-benzenedicarboxylate (bdc) linkers. Each side of this metal-oxo segment is terminated with two water molecules and one hydroxyl group. To simplify further the model cluster, we replaced the benzene rings from the bdc linkers by hydrogen atoms (Figure 3). Similar to the oxo-centered trimer, the MIL-53 type SBU has an overall charge of +1 that was neglected in the UFF calculations, but considered in the DFT calculations (see Supporting Information).

In order to avoid the introduction of too many UFF4MOF parameters, the octahedrally coordinated metal sites in the SBU of MIL-53 were described by using the M_6+3 atom types parametrized for the oxo-centered trimers (see Section 3.2), and the light elements were treated by applying the standard UFF atom types O_2, C_R and H_. We used the same (single) bond order for the M−O_{carb} and M−O_{hyd} bonds, considering their similar length in the reference crystal structures, and, as usual, we treated C−H and C−O_{carb} as single and resonant bonds respectively (Figure 3a). The UFF calculated and the experimentally determined structural characteristics of all studied MIL-53 SBUs are summarized in Table 4.

For all M^{III} ions, the UFF calculations slightly overestimate the M−M distance and the M−O_{carb} and M−O_{hyd} bonds, yielding maximum errors of less than 4% with respect to experiment. The standard Cr6+3 parameter yields a model cluster with greatly elongated Cr−Cr, Cr−O_{carb}, and Cr−O_{hyd} distances compared to those predicted by the use of Cr6f3, and the respective deviation from the experimental benchmark increases to 6.5%. For Al^{III}, Sc^{III} and Fe^{III}, UFF predicts more acute M−O_{hyd}−M and more obtuse M−O_{carb}−C angles, while

dx.doi.org/10.1021/ct400952t | J. Chem. Theory Comput. 2014, 10, 880−891

Table 4. UFF Derived Structural Characteristics (Bond Lengths and Angles), Experimental Reference Data in Parentheses, and Calculated Maximum Percent Errors for the MIL-53 type SBU[a]

metal center	M−M [Å]	M−O_{carb} [Å]	M−O_{hyd} [Å]	M−O_{hyd}−M [deg]	O_{hyd}−M−O_{hyd} [deg]	M−O_{carb}−C [deg]
Al^{III}	3.42 (3.38)	1.98 (1.92)	1.94 (1.89)	123.9 (126.8)	180.0 (179.2)	134.7 (133.4)
Sc^{III}	3.64 (3.65)	2.16 (2.13)	2.11 (2.12/2.06)	119.5 (122.9)	180.0 (176.8)	136.3 (135.0)
Cr^{III}	3.48 (3.41)	2.02 (1.96)	1.98 (1.95)	122.7 (121.7)	180.0 (180.0)	135.1 (138.8)
Fe^{III}	3.55 (3.44)	2.08 (2.01)	2.04 (1.99)	121.4 (124.6)	180.0 (180.0)	135.7 (134.9)
max % error[b]	*3.20*	*3.48*	*2.65*	*−2.8*	*1.8*	*−2. 7*
for	**Fe**	**Fe**	**Al**	**Sc**	**Sc**	**Cr**

[a]Force field parameters employed were M_6+3 for *M* = Al, Sc, and Fe and Cr6f3 for Cr (UFF4MOF atom types, see Table 1), O_2 C_R and H_ (UFF atom types[29]); bond orders as shown in Figure 3a. Experimental reference values taken from refs 37b, 55, 37a, and 37c for Al, Sc, Cr, and Fe, respectively. [b]The maximum % errors are derived after calculating all % errors for the MIL-53 type SBUs. The % errors are calculated as $(X_{UFF}-X_{Experiment})/X_{Experiment} \times 100$, where X_{UFF} denotes the UFF-predicted and $X_{Experiment}$ denotes the experimental values of respective bond lengths and angles.

for Cr^{III}, the trend is just the opposite (Table 4). The absolute maximum deviation in the bond angles is less than 3%.

It is worth noting that reoptimization of the UFF4MOF parameters with respect to the experimental MIL-53 SBU structures results in no change of the covalent radius of Sc^{III} and slight decrease of the r_i values for the remaining metal types (3% for Al^{III} and Cr^{III} and 4.5% for Fe^{III}). Employing the reoptimized parameters reduces the maximum errors in M−M, M−O_{carb}, and M−O_{hyd} below 1.5%, and keeps the performance for bond angles essentially unchanged (see Supporting Information Table S1 for detailed data). However, in view of the reasonable results shown in Table 4, and the relatively minor improvement achieved with reoptimized r_i values, and with the aim to keep the number of UFF4MOF atom types as small as possible, we do not introduce new Al, Cr, and Fe parameters. Instead, we adopt the M_6+3 (and Cr6f3) atom types, as parametrized for the $M_3O(CO_2H)_6$ clusters, in the calculations of the MIL-53 frameworks.

Finally, comparison of the UFF data to DFT predicted (instead of experimental) structures results in larger discrepancy regarding all bond lengths of interest, with maximum errors reaching out 6−8%, all in the case of Fe^{III} (Supporting Information Table S3).

The combination of atom types and bond orders used to calculate the MIL-53 type SBUs was employed in periodic structure calculations of Cr-, Al-, and Fe-based MIL-53 representatives (see Section 3.6).

3.4. Paddlewheel SBUs. Paddlewheels (PWs) represent another well-known and extensively employed building block in MOF synthesis. Various combinations of PW SBUs and di- or polytopic organic linkers of different size and functionalization have been synthetically realized into frameworks, such as MOF-2[56] and MOF-505,[57] and have given rise to MOF families such as HKUST-1,[38a] DMOF-1,[39] and SURMOFs.[58] The PW crystal structure consists of two divalent metal ions, M^{II}, bridged by four carboxylate groups. In the HKUST-1 MOFs[38,59] and the 2D SURMOFs,[58a,60] each metal center has one unsaturated axial site, which can be occupied by solvent or guest molecules. This open axial sites can, however, be used to extend the 2D (SUR)MOF lattice in the third dimension via coordination of pillar linkers with basic nitrogen atoms, such as diazabicyclooctane (dabco) or bipyridine (bpy). The layer-pillar MOF structures incorporating dabco pillars belong to the DMOF-1 family (known also as dabco MOFs),[39,61] other representatives are their isomorphous counterparts with bpy instead of dabco pillars[62] and the 3D SURMOFs.[58b]

PW structures containing Ti,[63] V,[64] Cr,[59,65] Mn,[66] Fe,[67] Co,[68] Ni,[38c,69] Cu,[38a,58a,60,70] and Zn[38b,39,56,58b,61,69] have all been synthetically realized in the form of molecular clusters and/or framework materials and are therefore included in our training set. It is important to note that PWs typically have a special electronic ground state with spin centers on the metal sites that may couple in different ways. Thus, these systems are clearly difficult cases for a classical mechanics approach such as a force field. However, UFF4MOF includes parameters that give qualitatively correct PW structures in both unsaturated (without pillar linkers) and saturated (with pillar linkers) forms. Unsurprisingly, the largest error bars are obtained for this SBU type, however, the impact on the overall MOF geometry is minor due to some fortuitous error cancellation and the relatively small spatial extension of the PW unit.

In the parametrization, we employ both bare $M_2(CO_2H)_4$ and pyridine-capped $M_2(CO_2H)_4(C_5H_5N)_2$ PW model structures with reference to DFT optimized geometries. The model structures, including bond-order definitions, are shown in Figure 4.

A set of new atom types labeled M_4+2, for all M types except Ni was introduced to describe the M^{II} ions in the bare and pillared PWs. The M_4+2 parameters (Table 1) are characterized by a bond angle of 90°, coordination number of 4, and metal bond radius chosen with respect to a corresponding DFT-derived reference geometry. In the case of Ni^{II}, the covalent radius derived by our scanning procedure differs only by 0.02 Å from the existing Ni4+2 atom type, and thus, we do not add a new atom type for Ni. The nonmetal atoms in the PW SBUs were described by O_2, C_R, H_, and N_R from ref 29. Bond orders of 3/2, 1, and 1/2 were employed for the C−O, C−H, and M−O bonds, respectively (see Figure 4a,c). For the M−M distance and *M* = Ti, Mn, Fe, Co, Ni, Cu, and Zn, we used a bond order of 1/4, whereas for *M* = V and Cr, the bond order was increased to 3 and 4, respectively, for reflecting the triple and quadrupole character of the metal−metal bond in divanadium and dichromium PW complexes.[64,65] The UFF-predicted structural characteristics of bare and pyridine-capped PWs are presented in Tables 5 and 6, respectively, along with the maximum percent errors with respect to the reference geometries and the RMSEs.

For most of the considered M^{II} ions, UFF overestimates the M−M and M−O distances in the bare PWs as compared to the DFT reference calculations. The largest deviations from the DFT values are, however, obtained for contracted bonds in the $M_2(CO_2H)_4$ SBUs with *M* = Zn and Cr, and account to −8%. The difference between the UFF- and DFT-predicted valence

dx.doi.org/10.1021/ct400952t | J. Chem. Theory Comput. 2014, 10, 880−891

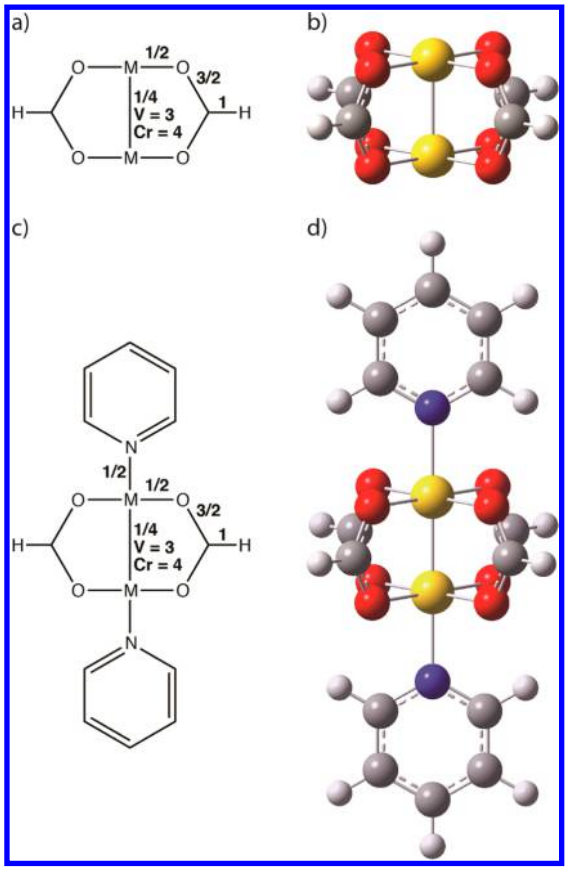

Figure 4. Left: Single-face schematic view of bare $M_2(CO_2H)_4$ (a) and pyridine-capped $M_2(CO_2H)_4(C_5H_5N)_2$ (c) paddlewheel type model clusters (PWs) with bond orders used in the UFF calculations. Right: Ball-and-stick representation of the structure of the bare (b) and pyridine-capped (d) PWs as predicted by UFF plus the UFF4MOF parameter extension. Color legend: divalent metal ions M yellow, O red, N blue, C gray, and H white. UFF atom types are given in Tables 5 and 6.

angles of interest is typically smaller in magnitude, and the maximum errors in O−M−O(*trans*) and O−M−M are almost twice as lower as those found for the bond lengths (see Table 5). In the pillared PW series, the largest errors in all UFF-derived structural characteristics are obtained also in the cases of Zn and Cr. As shown in Table 6, the M−M bond in $Zn_2(CO_2H)_4(C_5H_5N)_2$, and the M−O and M−N bonds in $Cr_2(CO_2H)_4(C_5H_5N)_2$ are largely underestimated by UFF in comparison to DFT. The 18% shorter Zn−Zn distance in the UFF-optimized Zn_2 pillared PW is coupled with a 6% reduction of the O−Zn−N angle, whereas the errors found for the other angles, O−Zn−O(*trans*) and O−Zn−Zn, reflect an overestimation of about 7%. It is important to note, that while the Zn−Zn bond is underestimated, the two axial Zn−N bonds are overestimated by UFF in comparison to DFT, and this compensating effect explains the fairly good performance of UFF in terms of predicted lattice parameters for the pillared DMOF-1(Zn) (see Section 3.6).

Much better agreement between UFF- and DFT-derived Zn−Zn distances in both bare and pillared Zn-paddlewheel SBUs could be achieved if partial charges of +2 per Zn atom and −0.5 per O atom are taken into account in the UFF model. In such calculations, the error drops down to about 4% for $Zn_2(CO_2H)_4$ and −9.6% for $Zn_2(CO_2H)_4(C_5H_5N)_2$. Employment of partial charges improves the M−M distance and most of the angles in the pillared PW with *M* = Cu as well but worsens the agreement with DFT in the case of the bare Cu_2 PW (see Tables S4 and S5 in the Supporting Information).

The comparison with already published DFT data for the M−M, M−O, and M−N distances in the $M_2(CO_2H)_4$ and $M_2(CO_2H)_4(C_5H_5N)_2$ SBUs is good, allowing for the different computational levels used (BP86/Slater basis set in our work, PBE/plane wave basis in ref 71 and B3LYP/Gaussian basis set in ref 72). In the case of the $M_2(CO_2H)_4$ clusters, the absolute difference in M−M distances calculated by us and Kim et al.[71] varies from 0.01 Å (for Ti, Mn, Co) up to 0.13 Å (for Cr). The Cu−Cu and Zn−Zn values derived from our calculations are underestimated by 0.02 and 0.04 Å, respectively, compared to the plane wave results in ref 71, and by 0.07 and 0.16 Å, respectively, compared to the hybrid-level data of Schmid et al.[72] For the pillared $M_2(CO_2H)_4(C_5H_5N)_2$ PWs, our DFT-optimized M−M values are typically shorter in comparison to those reported in refs 71 and 72. The underestimation with

Table 5. UFF Derived Structural Characteristics (Bond Lengths and Angles), DFT Reference Data in Parentheses, and Calculated Maximum Percent Errors and RMSE for Bare $M_2(CO_2H)_4$ Paddlewheel SBUs[a]

metal center	*M* (DFT)[c]	M−M [Å]	M−O [Å]	O−M−O (*trans*) [deg]	O−M−M [deg]	C−O−M [deg]
Ti^{II}	1	2.60 (2.82)	2.12 (1.98)	170.5 (163.6)	85.3 (81.8)	123.4 (126.6)
V^{II}	1	2.09 (1.95)	1.91 (2.04)	177.4 (171.2)	91.3 (94.5)	119.3 (112.8)
Cr^{II}	1	1.96 (1.82)	1.83 (1.98)	174.3 (167.7)	92.9(96.2)	118.6 (112.3)
Mn^{II}	7	2.46 (2.54)	1.99 (1.94)	173.6 (172.4)	86.7 (86.2)	122.2 (120.4)
Fe^{II}	5	2.34 (2.19)	1.84 (1.92)	176.5 (177.2)	88.2 (91.4)	121.1 (115.6)
Co^{II}	1	2.28 (2.21)	1.91 (1.90)	177.9 (178.1)	88.9 (91.0)	120.8 (115.7)
Ni^{II}	3	2.39 (2.32)	1.91 (1.94)	175.3 (179.2)	87.6 (89.6)	121.6 (116.2)
Cu^{II}	3	2.49 (2.47)	2.04 (1.98)	173.0 (175.2)	86.5 (88.0)	122.4 (117.6)
Zn^{II}	1	2.34 (2.54)	2.08 (2.04)	176.6 (173.2)	88.3 (86.6)	121.3 (119.0)
max % error[b]		*−7.87*	*−7.58*	*4.2*	*4.3*	*5.8*
for		**Zn**	**Cr**	**Ti**	**Ti**	**V**
RMSE		*0.14*	*0.09*	*4.3*	*2.5*	*4.8*

[a]Force field parameters employed were M_4+2 for *M* = Ti^{II}, V^{II}, Cr^{II}, Mn^{II}, Fe^{II}, Co^{II}, Cu^{II} and Zn^{II} (UFF4MOF atom types, see Table 1), Ni4+2 for Ni^{II}, O_2, C_R and H_ (UFF atom types[29]); bond orders as shown in Fig. 4a. [b]The maximum % errors are derived after calculating all % errors for the $M_2(CO_2H)_4$ series. The % errors are calculated as $(X_{UFF} - X_{DFT})/X_{DFT} \times 100$, where X_{UFF} denotes the UFF-predicted and X_{DFT} denotes the DFT-predicted value of respective bond lengths and angles. [c]*M* is the multiplicity of the $M_2(CO_2H)_4$ paddlewheel SBU, as used in the respective DFT calculation, and is given by the relation $M = 2S + 1$, where *S* is the total spin of the system.

dx.doi.org/10.1021/ct400952t | J. Chem. Theory Comput. 2014, 10, 880−891

Table 6. UFF Derived Structural Characteristics (Bond Lengths and Angles), DFT Reference Data in Parentheses, and Calculated Maximum Percent Errors and RMSE for Pillared $M_2(CO_2H)_4(C_5H_5N)_2$ Paddlewheel SBUs[a]

metal center	M (DFT)[c]	M−M [Å]	M−O [Å]	M−N [Å]	O−M−O (*trans*) [deg]	O−M−M [deg]	C−O−M [deg]	O−M−N [deg]
Ti^{II}	5	2.54 (2.63)	2.11 (2.08)	2.22 (2.25)	172.4 (170.1)	86.1 (85.0)	122.6 (122.1)	93.9 (95.0)
V^{II}	3	2.11 (2.20)	1.91 (2.03)	2.03 (2.34)	178.0 (178.3)	91.0 (90.9)	119.7 (116.7)	89.0 (89.1)
Cr^{II}	1	1.97 (1.87)	1.84 (2.00)	1.97 (2.49)	175.9 (169.2)	92.0 (95.4)	118.5 (112.9)	87.9 (84.6)
Mn^{II}	7	2.42 (2.40)	1.99 (2.06)	2.10 (2.02)	174.7 (176.8)	87.3 (88.4)	121.7 (117.9)	92.7 (91.6)
Fe^{II}	5	2.33 (2.17)	1.85 (2.00)	1.96 (2.16)	176.7 (177.3)	88.4 (91.4)	121.0 (115.6)	91.7 (88.6)
Co^{II}	1	2.28 (2.34)	1.92 (1.92)	2.04 (2.07)	178.1 (178.4)	89.0 (89.2)	120.8 (116.9)	91.0 (90.8)
Ni^{II}	3	2.37 (2.44)	1.91 (1.97)	2.02 (2.15)	175.9 (175.6)	87.9 (87.8)	121.3 (117.7)	92.1 (92.2)
Cu^{II}	3	2.45 (2.60)	2.04 (2.01)	2.14 (2.21)	174.2 (171.4)	87.1 (85.7)	121.8 (119.7)	92.9 (94.3)
Zn^{II}	1	2.31 (2.82)	2.08 (2.08)	2.19 (2.08)	177.4 (165.3)	88.7 (82.7)	121.0 (122.9)	91.3 (97.3)
max % error[b]		*−18.09*	*−7.86*	*−20.88*	*7.3*	*7.3*	*5.0*	*−6.2*
for		**Zn**	**Cr**	**Cr**	**Zn**	**Zn**	**Cr**	**Zn**
RMSE		*0.20*	*0.09*	*0.22*	*4.8*	*2.6*	*3.7*	*2.6*

[a]Force field parameters employed were M_4+2 for M = Ti^{II}, V^{II}, Cr^{II}, Mn^{II}, Fe^{II}, Co^{II}, Cu^{II}, and Zn^{II} (UFF4MOF atom types, see Table 1), Ni4+2 for Ni^{II}, O_2, C_R, and H_ (UFF atom types[29]); bond orders as shown in Figure 4c. [b]The maximum % errors are derived after calculating all % errors for the $M_2(CO_2H)_4(C_5H_5N)_2$ series. The % errors are calculated as $(X_{UFF} - X_{DFT})/X_{DFT} \times 100$, where X_{UFF} denotes the UFF-predicted and X_{DFT} denotes the DFT-predicted value of respective bond lengths and angles. [c]M is the multiplicity of the $M_2(CO_2H)_4(C_5H_5N)_2$ paddlewheel SBU, as used in the respective DFT calculation, and is given by the relation $M = 2S + 1$, where S is the total spin of the system.

respect to the plane waves data[71] ranges from −0.01 Å (for Ni) up to −0.5 Å (for Cr and Fe) and −0.67 Å (for V), and in the case of Cu and Zn PWs accounts to −0.04 and −0.02 Å, respectively. The difference with respect to the B3LYP results in ref 72 is larger and accounts to −0.11 and −0.15 Å for Cu−Cu and Zn−Zn, respectively. At the same time, the predictions for the M−O bonds in the bare PWs with Cu and Zn, and for the M−N distances in the pillared Cu_2 and Zn_2 PWs, as obtained in our work and in ref 72 are very similar, with absolute deviations in the range 0.01−0.02 Å.

The resulting atom types and bond orders were used to simulate the structures of several HKUST-1 and DMOF-1 representatives, and of the $Ni_2(bdc)_2(dabco)$ MOF (see Section 3.6).

3.5. MFU-4 Type SBU. The recently emerged family of MFU-4 frameworks[40] is attractive for its selective gas sorption properties.[73] The SBU of MFU-4, known also as "Kuratowski-type SBU",[74] contains Zn^{II} and/or Co^{II} centers with different coordination. The central metal site has octahedral configuration and is coordinated to six triazolate ligands, which in turn connect four tetrahedrally coordinated metal sites. The tetrahedral coordination environment of the latter is fulfilled by a capping chlorine ligand; see Figure 5.

Considering the specificity of this SBU, and in order to avoid overparameterization, we employed the following combination of atom types to describe the cluster: Zn3f2 (as parametrized for the Zn_4O SBU) to describe the tetrahedral Zn^{II} ions, Zn_{tet}, and Zn4+2 and Co4+2 (as parametrized for the respective Zn- and Co-containing paddlewheel SBUs) to describe the octahedral Zn^{II} and Co^{II} central sites, Zn_{oct} and Co_{oct}. For the tetrahedrally coordinated Co^{II} ions, Co_{tet}, a new atom type Co3+2, with r_i = 1.24 Å, θ_0 = 109.47° and coordination number = 4 (Table 1), was introduced in view of the experimental geometry of MFU-4(Co) and MFU-4*l*(Co_4Zn).[40b] For the light elements, we used the standard UFF atom types C_R, N_R, Cl, and H_. Bonds were described using bond orders of 1/2 for M_{tet}−N, 1 for M_{tet}−Cl, M_{oct}−N, and C−H, and 3/2 for the remaining resonant bonds (see Figure 5a).

The UFF performance is illustrated in Table 7 for selected bond lengths and angles of the SBU of MFU-4*l*(Co_4Zn). Obviously, the agreement with the experimental benchmark is

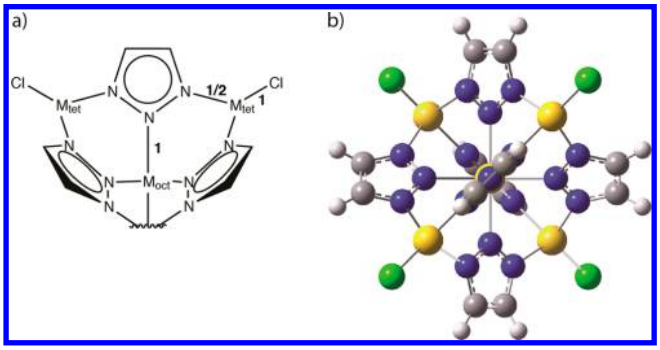

Figure 5. (a) Single-face schematic view of the Kuratowski-type model cluster with bond orders used in the UFF calculations. M_{tet} and M_{oct} indicate divalent metal ions with tetraherdal and octahedral coordination, respectively. (b) Ball-and-stick representation of the structure of the Kuratowski-type SBU as predicted by UFF plus the UFF4MOF parameter extension. Color legend: M_{tet} and M_{oct} (Zn or Co) yellow, N blue, C gray, Cl green, and H white. UFF atom types are given in Table 7.

Table 7. UFF Derived Structural Characteristics (Bond Lengths and Angles), Experimental Reference Data[40b] and Calculated Percent Errors for the Kuratowski-type SBU of MFU-4*l*(Co_4Zn)[a]

selected structural characteristics	UFF	experiment[b]	% error w.r.t. experiment[c]
Zn_{oct}−N [Å]	2.17	2.14	1.40
Co_{tet}−N [Å]	2.01	2.00	0.50
Co_{tet}−Cl [Å]	2.01	2.01	0.00
N−Zn_{oct}−N [deg]	90.0	90.0	0.0
N−Co_{tet}−N [deg]	101.2	97.6	3.7
N−Co_{tet}−Cl [deg]	116.9	119.6	−2.3

[a]Force field parameters employed were Co3+2 and Zn3f2 for M_{tet} = Co^{II} and Zn^{II}, resp., and M_4+2 for M_{oct} = Zn^{II} (UFF4MOF atom types, see Table 1), C_R, N_R, Cl, and H_ (UFF atom types[29]); bond orders as shown in Figure 5a. (M_{oct} is Zn^{II}, M_{tet} is Co^{II}). [b]Taken from ref 40b. [c]Calculated as $(X_{UFF} - X_{Experiment})/X_{Experiment} \times 100$ where X_{UFF} denotes UFF-predicted and $X_{Experiment}$ denotes experimental values of respective bond lengths and angles.

dx.doi.org/10.1021/ct400952t | J. Chem. Theory Comput. 2014, 10, 880−891

Table 8. Comparison of UFF Calculated and Experimentally Determined Cell Parameters of Selected MOFs[a]

MOF name	cell param. (Å) UFF	cell param. (Å) experimental[b]	% error[c]	crystal system (space group)	reference
MOF-5	$a = b = c = 26.08$	$a = b = c = 25.8849$	0.8	cubic ($Fm\bar{3}m$)	35a
IRMOF-8	$a = b = c = 30.34$	$a = b = c = 30.0915$	0.8		35b
IRMOF-10	$a = b = c = 34.77$	$a = b = c = 34.281$	1.4		35b
IRMOF-14	$a = b = c = 34.52$	$a = b = c = 34.381$	0.4		35b
IRMOF-16	$a = b = c = 43.64$	$a = b = c = 42.9806$	1.5	cubic ($Pm\bar{3}m$)	35b
MOF-177	$a = b = 37.65$	$a = b = 37.072$	1.6	hexagonal ($P31c$)	36
	$c = 30.51$	$c = 30.033$	1.6		
	($\gamma = 120°$)	($\gamma = 120°$)			
MOF-235(Fe)	$a = b = 12.74$	$a = b = 12.531$	1.7	hexagonal ($P62c$)	41
	$c = 18.78$	$c = 18.476$	1.6		
	($\gamma = 120°$)	($\gamma = 120°$)			
MIL-53(Cr)	$a = 6.60$	$a = 6.812$	−3.1	orthorhombic ($Imma$)	37a
	$b = 16.48$	$b = 16.733$	−1.5		
	$c = 12.66$	$c = 13.038$	−2.9		
MIL-53(Al)	$a = 6.51$	$a = 6.608$	−1.5		37b
	$b = 16.25$	$b = 16.675$	−2.5		
	$c = 12.49$	$c = 12.813$	−2.5		
MIL-53(Fe)	$a = 15.62$	$a = 15.9624$	−2.1	orthorhombic ($Imcm$)	37c
	$b = 13.98$	$b = 14.3920$	−2.9		
	$c = 6.61$	$c = 6.9351$	−4.7		
HKUST-1(Cu)[d]	$a = b = c = 26.94$	$a = b = c = 26.343$	2.3	cubic ($Fm\bar{3}m$)	38a
HKUST-1(Zn)	$a = b = c = 27.49$	$a = b = c = 26.520$	3.7		38b
HKUST-1(Ni)	$a = b = c = 26.48$	$a = b = c = 26.594$	−0.4		38c
DMOF-1(Zn)	$a = b = 11.31$	$a = b = 10.929$	3.5	tetragonal ($P4/mmm$)	39
	$c = 9.20$	$c = 9.608$	−4.2		
DMOF-1(Cu)[e]	$a = b = 11.08$				
	$c = 9.06$				
$Ni_2(bdc)_2(dabco)$	$a = b = 21.40$	$a = b = 21.593$	−0.90	trigonal ($P\bar{3}m1$)	38c
	$c = 8.95$	$c = 9.3672$	−4.5		
	($\gamma = 120°$)	($\gamma = 120°$)			
MFU-4(Zn)	$a = b = c = 21.62$	$a = b = c = 21.6265$	−0.03	cubic ($Fm\bar{3}m$)	40a
MFU-4l(Co_4Zn)	$a = b = c = 31.18$	$a = b = c = 30.995$	−0.6	cubic ($Fd\bar{3}m$)	40b
MFU-4(Co)	$a = b = c = 20.98$	$a = b = c = 21.731$	−3.5		40b

[a]Also shown are the calculated percent errors for the predicted with respect to the experimental lattice parameters, and the crystal systems and space groups taken from the corresponding references. [b]Experimental lattice parameters for desolvated MOF-5 and DMOF-1(Zn), as-synthesized IRMOFs 8, 10, 14, and 16, MOF-235, HKUST-1(Cu) and HKUST-1(Zn), MFU-4l(Co_4Zn), and MFU-4(Co), high temperature (ht) forms of MIL-53(Cr), MIL-53(Al), and MFU-4(Zn), open form of MIL-53(Fe), **1a** form of HKUST-1(Ni), and **3b** form of $Ni_2(bdc)_2(dabco)$ from ref 54. [c]Percent errors are calculated as $(X_{UFF} - X_{Experiment})/X_{Experiment} \times 100$, where X_{UFF} denotes UFF-predicted and $X_{Experiment}$ denotes experimental values of a, b, or c. [d]All HKUST-1 structures were calculated with water as axial ligands. [e]Single crystal experimental data are not available for DMOF-1(Cu), but its cell parameters should be comparable to those of DMOF-1(Zn), as the two compounds are isostructural.

excellent for the Co_{tet}−N and Co_{tet}−Cl bond lengths, as well as for the N−Zn_{oct}−N bond angle. The largest deviation is obtained for the angles characterizing the Co_{tet} centers, N−Co_{tet}−N, and N−Co_{tet}−Cl, and yet the calculated errors are below 4%. The comparison to the DFT structure is also reasonable (Table S6 in Supporting Information), with the exception of the Co_{tet}−Cl bond that is longer in the DFT model (2.13 Å) than the experimental value (2.01 Å), which is indeed excellently reproduced by the UFF (Table 7).

3.6. Application of UFF to Selected MOFs. In order to test the newly derived parameters, we apply them to 0 K, periodic constant-pressure geometry optimizations of a selection of well-known MOF structures for which experimental structural information is available. In each calculation, the atomic positions and lattice vectors are optimized simultaneously and the resultant cell parameters are shown in Table 8. Note that UFF employs a harmonic potential for bonded interactions; thus, we do not take temperature effects into account. All calculations were undertaken using GULP, which is space-group aware, however, we did not supply or constrain the space group in the calculations.

The agreement between calculated and experimental parameters is excellent, with only three of the calculated cell parameters having errors greater than 4%. The first of these errors is a 4.7% underestimation of the c dimension of MIL-53(Fe). The other two errors correspond to the c dimension of the pillar MOFs DMOF-1(Zn) and $Ni_2(bdc)_2(dabco)$, where cancellation of errors between the metal−metal, $r(M_{PW}-M_{PW})$ and metal−nitrogen, $r(M_{PW}-N_{pillar})$ distances is incomplete.

Accordingly, agreement with other, more expensive, computational approaches is also excellent. In particular, our UFF4MOF parameters yield comparable ground-state structures to force fields specifically designed for individual MOFs. Our computed lattice parameter of 26.08 Å for MOF-5, is equal to that gained by MOF-FF[27] and only slightly larger than the values of 25.95 Å[22a] and 26.04 Å[22b] obtained by Tafipolsky's

MOF-5 force fields. Similarly, for MIL-53(Al), we obtain cell parameters in close agreement to those given by the force field derived for that MOF (a = 17.05, b = 6.59, c = 12.91) by Vanduyfhuys et al.[24]

The excellent agreement of our computed lattice parameters, in an extension to a widely implemented force field, the Universal Force Field, supports the use of such a straightforward method to rapidly obtain geometries for comparison with experimental data and as a starting point for detailed computational investigation of MOF properties.

3.7. Performance of UFF4MOF beyond MOFs. The UFF4MOF extension provides transition metal parameters with coordination numbers that were not included in the original UFF paper.[29] Thus, it is an obvious question of whether our parameter extension may serve to treat systems that have been beyond the range of applicability of UFF. Without claiming here that UFF4MOF would complete UFF to cover all transition metal complexes known in inorganic and metal−organic chemistry, we test the performance for selected transition metal complexes with H_2O, CN^-, and NH_3 ligands (see Table 9). The results indicate that indeed the parameters

Table 9. Comparison between UFF4MOF Derived and DFT Calculated Bond Lengths for Hexacoordinated Complexes of Divalent and Trivalent Transition Metal Ions with H_2O, CN^-, or NH_3 Ligands[a]

			M−X [Å][c]	
metal center	coordination complex	multiplicity, M (DFT)[b]	UFF	DFT
V^{II}	$[V(H_2O)_6]^{2+}$	4	2.06	2.15
Mn^{II}	$[Mn(H_2O)_6]^{2+}$	2	2.05	2.06−2.07
Fe^{II}	$[Fe(H_2O)_6]^{2+}$	1	2.08	2.00−2.02
V^{II}	$[V(CN)_6]^{4-}$	4	2.17	2.26
Fe^{II}	$[Fe(CN)_6]^{4-}$	1	1.96	1.96
Co^{III}	$[Co(CN)_6]^{3-}$	1	2.03	1.92
V^{III}	$[V(NH_3)_6]^{3+}$	3	2.15	2.19−2.21
Cr^{III}	$[Cr(NH_3)_6]^{3+}$	4	2.11	2.15
Co^{II}	$[Co(NH_3)_6]^{2+}$	4	2.02	2.22−2.24

[a]UFF4MOF parameters employed were M_4+2 for M = V^{II}, Mn^{II}, Fe^{II} and Co^{II}, V_6+3 for V^{III} and Cr6f3 for Cr^{III}; standard UFF parameters[29] employed were Co6+3 for Co^{III}, O_2, C_R, N_R, and H_ ; bond orders employed were 1/2 for all metal-ligand bonds and 1 for all remaining bond types. [b]M is the multiplicity of the metal coordination complex, as used in the respective DFT calculation, and is given by the relation $M = 2S + 1$, where S is the total spin of the system. [c]X stands for oxygen atoms in the case of H_2O ligands, carbon atoms in the case of CN^- ligands and nitrogen atoms in the case of NH_3 ligands.

show a reasonable agreement with DFT calculations. We thus conclude that the parameters can be safely included in geometry preoptimizers that assign UFF parameters to atoms based on their coordination numbers. The treatment of real systems incorporating such transition metals may also be possible but will require careful validation prior to application.

4. CONCLUSION

We have extended and validated the Universal Force Field (UFF) for metal−organic frameworks and other framework compounds. Without changing the force field definition, it is possible to predict the structures of these materials at a surprisingly satisfactory level. For the organic linkers, existing UFF parameters give excellent results provided that chemically reasonable bond orders are employed. For the inorganic units, it was necessary to extend the original UFF parameter set by 18 additional atom types. These UFF4MOF parameters have been fit at the SBU level, and validated for periodic calculations, yielding very good agreement with experiment. UFF with the reported parameter extension has been applied to calculate the structure of several representative periodic MOFs. We conclude that the performance of UFF using the UFF4MOF parameters is satisfactory to predict MOF structures, including hypothetical new MOFs, with a large range of transition metals included in the inorganic building blocks. The method will be useful for screening MOF structures for selected applications, for providing structures for visual analysis or as starting point for more sophisticated simulations. The parameter extensions and recommended bond orders are provided in this article. The UFF4MOF parameter extension is available in GULP,[43] deMonNano,[42] and ADF,[44c] and it is straightforward to include them in any existing UFF implementation.

■ ASSOCIATED CONTENT

Supporting Information

All scan data for each SBU; UFF and DFT geometries for common organic linker molecules; reoptimization of octahedral metal parameters with respect to the MIL-53 series of SBUs; reoptimization of the Zn parameter for the Zn_4O SBU using GULP; comparison of UFF and DFT predicted structures for trimeric, MIL-53 and Kuratowski-type SBUs; comparison of UFF and DFT predicted structures for the paddlewheel SBUs with partial charges considered in the UFF calculations. This information is available free of charge via the Internet at http://pubs.acs.org

■ AUTHOR INFORMATION

Corresponding Author

*E-mail: t.heine@jacobs-university.de.

Author Contributions

[†]M.A.A. and N.V. contributed equally.

Notes

The authors declare no competing financial interest.

■ ACKNOWLEDGMENTS

This work has been financially supported by the European Commission through the European Research Council (ERC StG C3ENV GA 256962), the Marie Curie Actions (MC-IIF GA-MOF, GA 327758, and MC-IAPP QUASINANO, GA 251149) and by Solvay GmbH.

■ REFERENCES

(1) O'Keeffe, M.; Peskov, M. a.; Ramsden, S. J.; Yaghi, O. M. *Acc. Chem. Res.* **2008**, *41*, 1782−9.

(2) Yaghi, O. M.; O'Keeffe, M.; Ockwig, N. W.; Chae, H. K.; Eddaoudi, M.; Kim, J. *Nature* **2003**, *423* (6941), 705−714.

(3) (a) Suh, M. P.; Park, H. J.; Prasad, T. K.; Lim, D.-W. *Chem. Rev.* **2012**, *112*, 782−835. (b) Sumida, K.; Rogow, D. L.; Mason, J. A.; McDonald, T. M.; Bloch, E. D.; Herm, Z. R.; Bae, T.-H.; Long, J. R. *Chem. Rev.* **2011**, *112* (2), 724−781. (c) Li, J.-R.; Sculley, J.; Zhou, H.-C. *Chem. Rev.* **2011**, *112* (2), 869−932. (d) Czaja, A. U.; Trukhan, N.; Muller, U. *Chem. Soc. Rev.* **2009**, *38* (5), 1284−1293. (e) Almeida Paz, F. A.; Klinowski, J.; Vilela, S. M. F.; Tome, J. P. C.; Cavaleiro, J. A. S.; Rocha, J. *Chem. Soc. Rev.* **2012**, *41* (3), 1088−1110. (f) Jiang, H.-L.; Xu, Q. *Chem. Commun.* **2011**, *47* (12), 3351−3370.

(4) Yoon, M.; Srirambalaji, R.; Kim, K. *Chem. Rev.* **2012**, *112*, 1196−231.

(5) (a) Zhang, W.; Xiong, R.-G. *Chem. Rev.* **2012**, *112*, 1163−95. (b) Kurmoo, M. *Chem. Soc. Rev.* **2009**, *38* (5), 1353−1379.
(6) (a) Kreno, L. E.; Leong, K.; Farha, O. K.; Allendorf, M.; Van Duyne, R. P.; Hupp, J. T. *Chem. Rev.* **2012**, *112*, 1105−25. (b) Cui, Y.; Yue, Y.; Qian, G.; Chen, B. *Chem. Rev.* **2012**, *112*, 1126−62.
(7) (a) Bétard, A.; Fischer, R. A. *Chem. Rev.* **2012**, *112*, 1055−83. (b) Shekhah, O.; Liu, J.; Fischer, R. A.; Woll, C. *Chem. Soc. Rev.* **2011**, *40* (2), 1081−1106.
(8) Yamada, T.; Otsubo, K.; Makiura, R.; Kitagawa, H. *Chem. Soc. Rev.* **2013**, *42* (16), 6655−6669.
(9) Horcajada, P.; Gref, R.; Baati, T.; Allan, P. K.; Maurin, G.; Couvreur, P.; Férey, G.; Morris, R. E.; Serre, C. *Chem. Rev.* **2012**, *112*, 1232−68.
(10) (a) Wilmer, C. E.; Leaf, M.; Lee, C. Y.; Farha, O. K.; Hauser, B. G.; Hupp, J. T.; Snurr, R. Q. *Nat. Chem.* **2012**, *4*, 83−9. (b) Wilmer, C. E.; Snurr, R. Q. *Chem. Eng. J.* **2011**, *171*, 775−781.
(11) (a) Oliveira, A. F.; Seifert, G.; Heine, T.; Duarte, H. a. *J. Braz. Chem. Soc.* **2009**, *20*, 1193−1205. (b) Lukose, B.; Supronowicz, B.; St Petkov, P.; Frenzel, J.; Kuc, A. B.; Seifert, G.; Vayssilov, G. N.; Heine, T. *Phys. Status Solidi B* **2012**, *249* (2), 335−342. (c) Seifert, G.; Porezag, D.; Frauenheim, T. *Int. J. Quantum Chem.* **1996**, *58* (2), 185−192.
(12) Allinger, N. L. *J. Am. Chem. Soc.* **1977**, *99*, 8127−8134.
(13) Allinger, N. L.; Yuh, Y. H.; Lii, J. H. *J. Am. Chem. Soc.* **1989**, *111*, 8551−8566.
(14) Cornell, W. D.; Cieplak, P.; Bayly, C. I.; Gould, I. R.; Merz, K. M.; Ferguson, D. M.; Spellmeyer, D. C.; Fox, T.; Caldwell, J. W.; Kollman, P. A. *J. Am. Chem. Soc.* **1995**, *117*, 5179−5197.
(15) Brooks, B. R.; Bruccoleri, R. E.; Olafson, B. D.; States, D. J.; Swaminathan, S.; Karplus, M. *J. Comput. Chem.* **1983**, *4*, 187−217.
(16) Bueno-Pérez, R.; Calero, S.; Dubbeldam, D.; Ania, C. O.; Parra, J. B.; Zaderenko, A. P.; Merkling, P. J. *J. Phys. Chem. C* **2012**, *116*, 25797−25805.
(17) Zheng, J.; Balasundaram, R.; Gehrke, S. H.; Heffelfinger, G. S.; Goddard, W. A.; Jiang, S. *J. Chem. Phys.* **2003**, *118*, 5347.
(18) Marques, H. M.; Munro, O. Q.; Grimmer, N. E.; Levendis, D. C.; Marsicano, F.; Pattrick, G.; Markoulides, T. *J. Chem. Soc., Faraday Trans.* **1995**, *91* (12), 1741−1749.
(19) Marques, H. M.; Brown, K. L. *THEOCHEM* **1995**, *340*, 97−124.
(20) Autenrieth, F.; Tajkhorshid, E.; Baudry, J.; Luthey-Schulten, Z. *J. Comput. Chem.* **2004**, *25* (13), 1613−1622.
(21) Li, X. Y.; Czernuszewicz, R. S.; Kincaid, J. R.; Stein, P.; Spiro, T. G. *J. Phys. Chem.* **1990**, *94* (1), 47−61.
(22) (a) Tafipolsky, M.; Amirjalayer, S.; Schmid, R. *J. Comput. Chem.* **2007**, *28*, 1169−1176. (b) Tafipolsky, M.; Schmid, R. *J. Phys. Chem. B* **2009**, *113*, 1341−52.
(23) Tafipolsky, M.; Amirjalayer, S.; Schmid, R. *J. Phys. Chem. C* **2010**, *114*, 14402−14409.
(24) Vanduyfhuys, L.; Verstraelen, T.; Vandichel, M.; Waroquier, M.; Van Speybroeck, V. *J. Chem. Theory Comput.* **2012**, *8*, 3217−3231.
(25) Amirjalayer, S.; Tafipolsky, M.; Schmid, R. *Angew. Chem., Int. Ed. Engl.* **2007**, *46*, 463−6.
(26) (a) Getman, R. B.; Miller, J. H.; Wang, K.; Snurr, R. Q. *J. Phys. Chem. C* **2010**, *115* (5), 2066−2075. (b) Han, S. S.; Choi, S.-H.; Goddard, W. A. *J. Phys. Chem. C* **2010**, *114* (27), 12039−12047.
(27) Bureekaew, S.; Amirjalayer, S.; Tafipolsky, M.; Spickermann, C.; Roy, T. K.; Schmid, R. *Phys. Status Solidi B* **2013**, *250*, 1128−1141.
(28) Mayne, C. G.; Saam, J.; Schulten, K.; Tajkhorshid, E.; Gumbart, J. C. *J. Comput. Chem.* **2013**, *34*, 2757−2770.
(29) Rappe, A. K.; Casewit, C. J.; Colwell, K. S.; Goddard, W. A.; Skiff, W. M. *J. Am. Chem. Soc.* **1992**, *114*, 10024−10035.
(30) Liu, L.; Liu, Y.; Zybin, S. V.; Sun, H.; Goddard, W. A. *J. Phys. Chem. A* **2011**, *115*, 11016−22.
(31) Casewit, C. J.; Colwell, K. S.; Rappe, A. K. *J. Am. Chem. Soc.* **1992**, *114*, 10046−10053.
(32) Casewit, C. J.; Colwell, K. S.; Rappe, A. K. *J. Am. Chem. Soc.* **1992**, *114*, 10035−10046.
(33) Rappe, A. K.; Colwell, K. S.; Casewit, C. J. *Inorg. Chem.* **1993**, *32*, 3438−3450.
(34) (a) García-Peérez, E.; Gascón, J.; Morales-Flórez, V. c.; Castillo, J. M.; Kapteijn, F.; Calero, S. a. *Langmuir* **2009**, *25* (3), 1725−1731. (b) Pachfule, P.; Chen, Y.; Sahoo, S. C.; Jiang, J.; Banerjee, R. *Chem. Mater.* **2011**, *23* (11), 2908−2916. (c) Surblé, S.; Millange, F.; Serre, C.; Düren, T.; Latroche, M.; Bourrelly, S.; Llewellyn, P. L.; Férey, G. *J. Am. Chem. Soc.* **2006**, *128* (46), 14889−14896. (d) Wang, S.; Yang, Q.; Zhong, C. *Sep. Purif. Technol.* **2008**, *60* (1), 30−35.
(35) (a) Li, H.; Eddaoudi, M.; O'Keeffe, M.; Yaghi, O. M. *Nature* **1999**, *402* (6759), 276−279. (b) Eddaoudi, M.; Kim, J.; Rosi, N.; Vodak, D.; Wachter, J.; O'Keeffe, M.; Yaghi, O. M. *Science (New York, N.Y.)* **2002**, *295*, 469−72.
(36) Chae, H. K.; Siberio-Perez, D. Y.; Kim, J.; Go, Y.; Eddaoudi, M.; Matzger, A. J.; O'Keeffe, M.; Yaghi, O. M. *Nature* **2004**, *427* (6974), 523−527.
(37) (a) Millange, F.; Serre, C.; Férey, G. *Chem. Commun.* **2002**, 822−3. (b) Loiseau, T.; Serre, C.; Huguenard, C.; Fink, G.; Taulelle, F.; Henry, M.; Bataille, T.; Férey, G. *Chemistry* **2004**, *10*, 1373−82. (c) Millange, F.; Guillou, N.; Medina, M. E.; Férey, G. r.; Carlin-Sinclair, A.; Golden, K. M.; Walton, R. I. *Chem. Mater.* **2010**, *22*, 4237−4245.
(38) (a) Chui, S. S. *Science* **1999**, *283*, 1148−1150. (b) Feldblyum, J. I.; Liu, M.; Gidley, D. W.; Matzger, A. J. *J. Am. Chem. Soc.* **2011**, *133* (45), 18257−18263. (c) Maniam, P.; Stock, N. *Inorg. Chem.* **2011**, *50*, 5085−97.
(39) Dybtsev, D. N.; Chun, H.; Kim, K. *Angew. Chem., Int. Ed. Engl.* **2004**, *43* (38), 5033−5036.
(40) (a) Biswas, S.; Grzywa, M.; Nayek, H. P.; Dehnen, S.; Senkovska, I.; Kaskel, S.; Volkmer, D. *Dalton Trans* **2009**, 6487−95. (b) Denysenko, D.; Werner, T.; Grzywa, M.; Puls, A.; Hagen, V.; Eickerling, G.; Jelic, J.; Reuter, K.; Volkmer, D. *Chem. Commun.* **2012**, *48* (9), 1236−1238.
(41) Sudik, A. C.; Côté, A. P.; Yaghi, O. M. *Inorg. Chem.* **2005**, *44*, 2998−3000.
(42) deMonNano *deMonNano*; http://physics.jacobs-university.de/theine/research/deMon/, 2009.
(43) Gale, J. D. *GULP*, Version 4.08; http://projects.ivec.org/gulp/.
(44) (a) Fonseca Guerra, C.; Snijders, J. G.; te Velde, G.; Baerends, E. J. *Theor. Chim. Acta* **1998**, *99*, 391−403. (b) te Velde, G.; Bickelhaupt, F. M.; Baerends, E. J.; Fonseca Guerra, C.; van Gisbergen, S. J. A.; Snijders, J. G.; Ziegler, T. *J. Comput. Chem.* **2001**, *22*, 931−967. (c) ADF2012. *Theoretical Chemistry*; Vrije Universiteit: Amsterdam, The Netherlands, 2012. http://www.scm.com.
(45) (a) Becke, A. *Phys. Rev. A* **1988**, *38*, 3098−3100. (b) Perdew, J. P.; Yue, W. *Phys. Rev. B* **1986**, *33*, 8800−8802.
(46) van Lenthe, E.; Baerends, E. J. *J. Comput. Chem.* **2003**, *24*, 1142−56.
(47) (a) van Lenthe, E.; Baerends, E. J.; Snijders, J. G. *J. Chem. Phys.* **1993**, *99*, 4597. (b) van Lenthe, E.; Baerends, E. J.; Snijders, J. G. *J. Chem. Phys.* **1994**, *101*, 9783. (c) van Lenthe, E.; Ehlers, A.; Baerends, E.-J. *J. Chem. Phys.* **1999**, *110*, 8943.
(48) Volkringer, C.; Popov, D.; Loiseau, T.; Férey, G. r.; Burghammer, M.; Riekel, C.; Haouas, M.; Taulelle, F. *Chem. Mater.* **2009**, *21*, 5695−5697.
(49) Dietzel, P. D. C.; Blom, R.; Fjellvåg, H. *Dalton Trans.* **2006**, 2055−7.
(50) Lieb, A.; Leclerc, H.; Devic, T.; Serre, C.; Margiolaki, I.; Mahjoubi, F.; Lee, J. S.; Vimont, A.; Daturi, M.; Chang, J.-S. *Microporous Mesoporous Mater.* **2012**, *157*, 18−23.
(51) Figgis, B. N.; Robertson, G. B. *Nature* **1965**, *205*, 694−695.
(52) Li, J.; Yang, S. M.; Zhang, F. X.; Tang, Z. X.; Ma, S. L.; Shi, Q. Z.; Wu, Q. J.; Huang, Z. X. *Inorg. Chim. Acta* **1999**, *294* (1), 109−113.
(53) Shova, S. G.; Cadelnic, I. G.; Gdaniec, M.; Simonov, Y. A.; Jovmir, T. C.; Meriacre, V. M.; Filoti, G.; Turta, C. I. *J. Struct. Chem.* **1998**, *39* (5), 747−761.
(54) Cohen, S. M. *Chem. Rev.* **2012**, *112*, 970−1000.

(55) Mowat, J. P. S.; Miller, S. R.; Slawin, A. M. Z.; Seymour, V. R.; Ashbrook, S. E.; Wright, P. A. *Microporous Mesoporous Mater.* **2011**, *142* (1), 12−12.
(56) Li, H.; Eddaoudi, M.; Groy, T. L.; Yaghi, O. M. *J. Am. Chem. Soc.* **1998**, *120* (33), 8571−8572.
(57) Chen, B. L.; Ockwig, N. W.; Millward, A. R.; Contreras, D. S.; Yaghi, O. M. *Angew. Chem., Int. Ed. Engl.* **2005**, *44* (30), 4745−4749.
(58) (a) Shekhah, O.; Wang, H.; Zacher, D.; Fischer, R. A.; Wöll, C. *Angew. Chem., Int. Ed. Engl.* **2009**, *48* (27), 5038−5041. (b) Shekhah, O.; Wang, H.; Paradinas, M.; Ocal, C.; Schupbach, B.; Terfort, A.; Zacher, D.; Fischer, R. A.; Woll, C. *Nat. Mater.* **2009**, *8* (6), 481−484.
(59) Murray, L. J.; Dinca, M.; Yano, J.; Chavan, S.; Bordiga, S.; Brown, C. M.; Long, J. R. *J. Am. Chem. Soc.* **2010**, *132* (23), 7856−+.
(60) Liu, J.; Lukose, B.; Shekhah, O.; Arslan, H. K.; Weidler, P.; Gliemann, H.; Braese, S.; Grosjean, S.; Godt, A.; Feng, X.; Muellen, K.; Magdau, I.-B.; Heine, T.; Woell, C. *Sci. Rep.* **2012**, *2*, 921.
(61) Lee, J. Y.; Olson, D. H.; Pan, L.; Emge, T. J.; Li, J. *Adv. Funct. Mater.* **2007**, *17*, 1255−1262.
(62) Chun, H.; Dybtsev, D. N.; Kim, H.; Kim, K. *Chem.—Eur. J.* **2005**, *11* (12), 3521−3529.
(63) Mendiratta, A.; Cummins, C. C.; Cotton, F. A.; Ibragimov, S. A.; Murillo, C. A.; Villagrán, D. *Inorg. Chem.* **2006**, *45*, 4328−30.
(64) Cotton, F. A.; Hillard, E. a.; Murillo, C. a.; Wang, X. *Inorg. Chem.* **2003**, *42*, 6063−70.
(65) Cotton, F. A.; Daniels, L. M.; Murillo, C. A.; Pascual, I.; Zhou, H. C. *J. Am. Chem. Soc.* **1999**, *121* (29), 6856−6861.
(66) Fu, Z.; Yi, J.; Chen, Y.; Liao, S.; Guo, N.; Dai, J.; Yang, G.; Lian, Y.; Wu, X. *Eur. J. Inorg. Chem.* **2008**, *2008*, 628−634.
(67) Lee, D.; Bois, J. D.; Petasis, D.; Hendrich, M. P.; Krebs, C.; Huynh, B. H.; Lippard, S. J. *J. Am. Chem. Soc.* **1999**, *121*, 9893−9894.
(68) Benbellat, N.; Gavrilenko, K. S.; Le Gal, Y.; Cador, O.; Golhen, S.; Gouasmia, A.; Fabre, J.-M.; Ouahab, L. *Inorg. Chem.* **2006**, *45* (26), 10440−10442.
(69) Kounavi, K. A.; Manos, M. J.; Tasiopoulos, A. J.; Perlepes, S. P.; Nastopoulos, V. *Bioinorg. Chem. Appl.* **2010**, 178034.
(70) (a) Lin, X.; Telepeni, I.; Blake, A. J.; Dailly, A.; Brown, C. M.; Simmons, J. M.; Zoppi, M.; Walker, G. S.; Thomas, K. M.; Mays, T. J.; Hubberstey, P.; Champness, N. R.; Schröder, M. *J. Am. Chem. Soc.* **2009**, *131* (6), 2159−2171. (b) Ma, L.; Mihalcik, D. J.; Lin, W. *J. Am. Chem. Soc.* **2009**, *131* (13), 4610−4612.
(71) Bak, J. H.; Le, V.-D.; Kang, J.; Wei, S.-H.; Kim, Y.-H. *J. Phys. Chem. C* **2012**, *116*, 7386−7392.
(72) Bureekaew, S.; Amirjalayer, S.; Schmid, R. *J. Mater. Chem.* **2012**, *22*, 10249.
(73) (a) Denysenko, D.; Grzywa, M.; Tonigold, M.; Streppel, B.; Krkljus, I.; Hirscher, M.; Mugnaioli, E.; Kolb, U.; Hanss, J.; Volkmer, D. *Chem.—Eur. J.* **2011**, *17* (6), 1837−1848. (b) Teufel, J.; Oh, H.; Hirscher, M.; Wahiduzzaman, M.; Zhechkov, L.; Kuc, A.; Heine, T.; Denysenko, D.; Volkmer, D. *Adv. Mater. (Weinheim, Ger.)* **2013**, *25* (4), 635−639.
(74) Biswas, S.; Tonigold, M.; Speldrich, M.; Kögerler, P.; Weil, M.; Volkmer, D. *Inorg. Chem.* **2010**, *49*, 7424−34.